

INTRODUCTION

The oil and gas industry play a vital role in Nigeria's economy and the upstream oil sector is the single most important sector in the economy, accounting for over 90% of the country's exports and about 80% of the Federal Government (FG's) revenue as at 2017 (Michael, 2018).

average field recovery from water flooding is currently around 35%, leaving between 60 to 70% of oil in place, and this represents a substantial opportunity.

This study was done using an elaborate approach of geophysical interpretation, geological principles, statistical tools and uncertainty management techniques to recharacterize target reservoirs

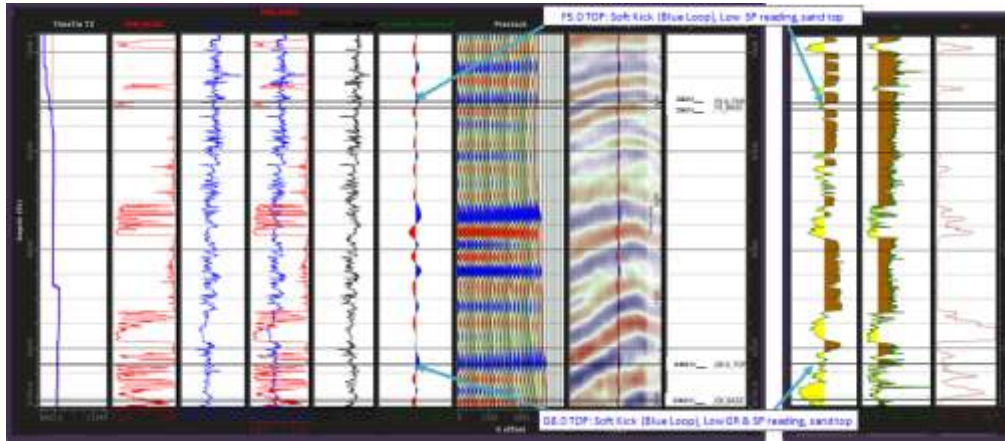


Figure 13: Reflectivity Pattern Analysis performed using nDI GEOSIGNS (ANTI-SEG convention adopted).

Natural resources have made Nigeria a wealthy nation. However, the oil fields in the onshore Nigeria are maturing and this development is a global trend in the western world, which has led to production optimization and increased outtake become even more important facing these new challenges.

The capital expenditure involved in a new field development is typically huge, many investment decisions are irreversible, and finance is committed for the long-term. Therefore, the oil companies rather invest in reservoir redevelopment. To meet rising demand, the oil and gas industry will have to maximize economic ultimate recovery from existing oil and gas fields. Global

GEOLOGY OF STUDY AREA

The OBOM field is one of the Niger Delta Oil fields, located on the south- eastern onshore part of the Nigerian's Oil concessions. It is in Greater Ughelli Depobelt aging from the Rupelian through the Chattian to the Aquitanian. It was discovered by an exploration well OBOM-001 1965. To date, 15 wells have been drilled with 14 of them completed at different intervals. The field is a simple roll-over structure elongated in the east-west direction and bounded by a curved main growth fault in the north and east. Some small crestal faulting exists for the reservoirs at the shallower depth, and at the deeper reservoirs,

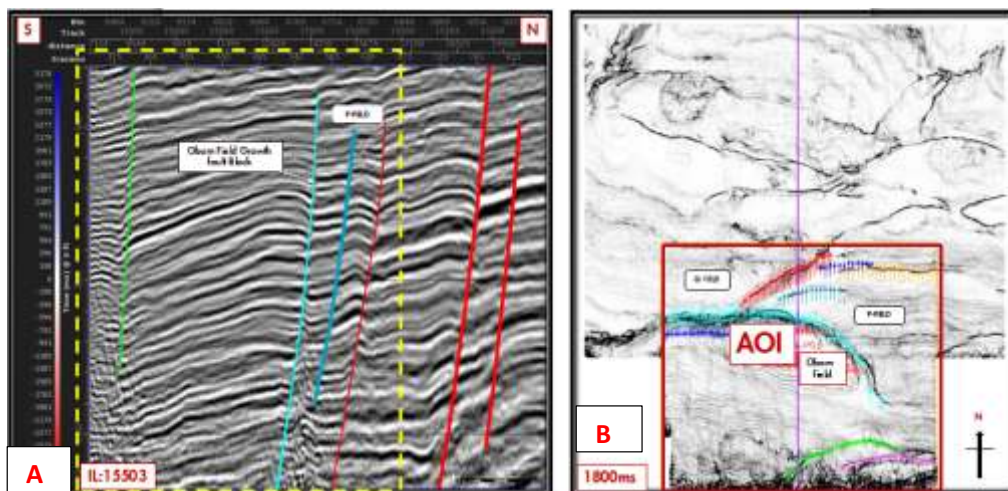


Figure 14: (A) Fault interpretation on inline section 15503 (B) Semblance for QC.

hydrocarbon accumulations are mainly dip closures for the shallower sands and dip-assisted fault closures for the deeper reservoirs.

The field is made of stacked paralic sequence of sand, silt and shale. The field has a total of 42 stacks of reservoirs penetrated between 6400-12900ftss. The sands of focus which are the G8000 and F5000 were deposited in lower Miocene to upper Oligocene in age respectively. The alternating sands, separated by field-wide shale units are interpreted to represent the delta front, distributary channels and the deltaic plain. The upper part has lower sandstone content than the lower part, demonstrating an overall depositional sequence that shows a transgressive marine setting with distal sediments overlying by proximal

sediments.

METHODOLOGY

The research reported here focuses on giving a detailed account of the various processes and steps taken to obtain results and prepare several work products used for analyses and arriving at the project objectives.

DATA REVIEW/INTERPRETATION

The data used for this study include a 3D seismic volume, 14 wells with gamma ray logs, resistivity logs, calliper logs, SP logs, paucity of neutron logs, and paucity of density logs which was mitigated by modelling density

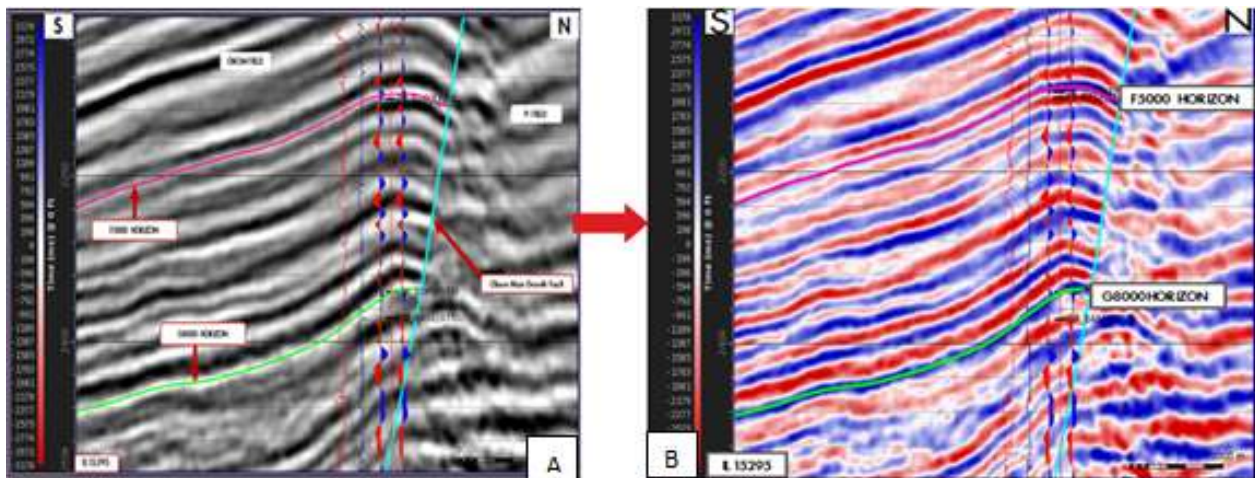


Figure 15: (A & B) F5000 (pink line) and G8000 (green line) horizons on Inline sections display mode in grey scale/variable density mode for emphasis of visual aid.

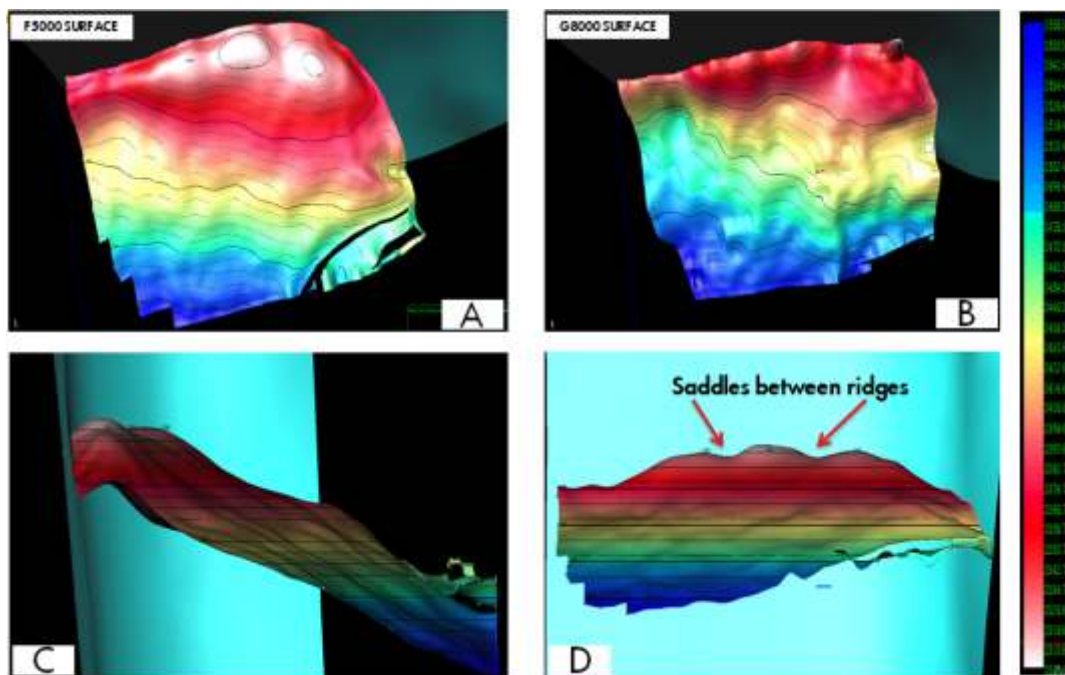


Figure 16: (A) F5000 surface (B) G8000 surface (C) Fault-horizon architecture (D) Surface showing saddles and ridges.

Table 2: Comparison of residuals associated with the three velocity models tested after depth conversion.

VoK MODEL					POLYNOMIAL FUNCTION MODEL					3D PSDM SEISMIC VELOCITY				
Reservoir	F5000		G8000		Reservoir	F5000		G8000		Reservoir	F5000		G8000	
Well	Before shift	After shift	Before shift	After shift	Well	Before shift	After shift	Before shift	After shift	Well	Before shift	After shift	Before shift	After shift
	Residual (ft)	Residual (ft)	Residual (ft)	Residual (ft)		Residual (ft)	Residual (ft)	Residual (ft)	Residual (ft)		Residual	Residual	Residual	Residual
Obom-001	174.902	-33.329	166.401	-65.129	Obom-001	-63.581	-31.16	-142.967	-64.1	Obom-001	108.297	-5.184	99.219	-35.626
Obom-002	164.894	-44.06	249.688	17.822	Obom-002	-74.806	-42.27	-60.331	18.655	Obom-002	59.754	-54.655	189.766	-54.828
Obom-003	234.992	25.189	224.708	-8.019	Obom-003	-6.617	26.052	-86.932	-7.648	Obom-003	162.576	48.164	131.378	-4.531
Obom-004	218.362	7.048	244.517	8.121	Obom-004	-26.989	5.923	-73.367	7.176	Obom-004	116.886	1.252	158.221	20.289
Obom-005	214.239	3.593	261.923	28.267	Obom-005	-29.48	3.324	-51.399	28.204	Obom-005	84.888	-30.773	173.85	37.477
Obom-006	261.037	51.674	231.809	2.182	Obom-006	20.549	53.147	-73.716	-4.495	Obom-006	115.9	0.712	60.747	-74.476
Obom-007	Outside	Outside	Outside	Outside	Obom-007	Outside	Outside	Outside	Outside	Obom-007	Outside	Outside	Outside	Outside
Obom-008	222.086	8.524	252.657	13.881	Obom-008	-28.499	4.773	-70.088	11.28	Obom-008	104.602	-12.472	127.178	-12.687
Obom-009	203.711	-6.717	267.28	31.887	Obom-009	-39.47	-6.7	-49.003	31.196	Obom-009	119.18	4.261	225.787	89.073
Obom-010	195.029	-15.057	241.847	6.737	Obom-010	-47.295	-14.58	-73.97	6.133	Obom-010	108.487	-6.273	75.739	-62.583
Obom-011	236.041	26.421	209.58	-25.585	Obom-011	-5.104	27.535	-106.328	-26.21	Obom-011	159.645	45.276	141.582	4.623
Obom-012	178.26	-33.265	218.496	-12.515	Obom-012	-67.596	-34.65	-89.853	-11.16	Obom-012	112.986	-2.256	119.067	-15.937
Obom-013	219.612	8.331	Outside	Null	Obom-013	-25.659	7.248	Outside	Null	Obom-013	126.545	11.046	Outside	Outside
	STD RES	26.02219	STD REES	27.49366		STD RES	27.939	STD REES	27.076		STD RES	26.07923	STD RES	48.93427
	Ave RES	-0.13733	Ave RES	-0.21373		Ave RES	-0.114	Ave RES	-0.18		Ave RES	-0.007317	Ave RES	0.004909
Scaling Factor (SC0)	1.02579	SC0	1.01737		Scaling Factor (SC0)	0.99610	SC0	0.99189		Scaling Factor (SC0)	1.01394	SC0	1.01422	

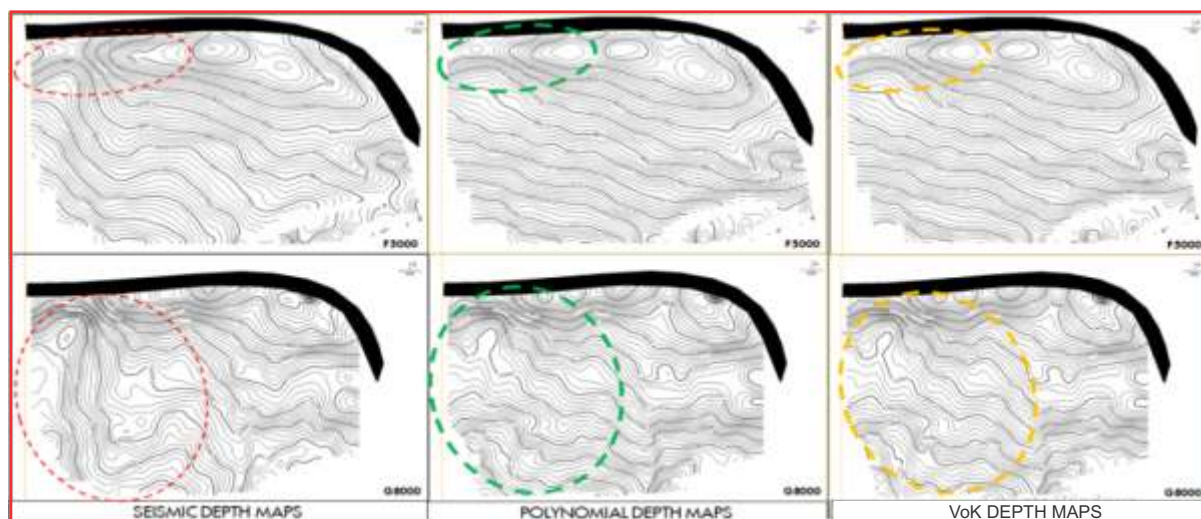


Figure 17: Depth maps from the 3 velocity models (VoK, Polynomial Function and Seismic velocity).

from spliced SP-GR logs.

3D SEISMIC & WELL DATA ANALYSIS FOR OBOM FIELD

The OBOM seismic survey covers 100sq. km acquired in the inline direction (North-South trend) on a shot-receiver grid density of 50m x 50m, processed in a grid of 25m x 25m bin cell size at a 2ms sample rate and has a 15-fold coverage. Prior to structural interpretation, two seismic

vintages available from the field were analysed with aim to achieve the volume with substantially improved imaging, good signal quality and resolution. The reprocessed 3D PreStack Time/Depth Migrated volume of 2016 improvement over the first processed PoStack Time migrated volume of 1994 was seen in the sharp fault plane definition, clearer reflector continuity and good imaging in front and behind faults, as well deep in reflectors (Figure 3a). In order to enhance S/N ratio, post processing - Van Gogh filtering was applied to suppress

Table 3: showing the Depth Uncertainty.

Reservoir	Average Depth	Depth Uncertainty Value Advised	Data Points
F5000	8367.46	34.01	13 Wells
G8000	9737.84	44.65	11 Wells

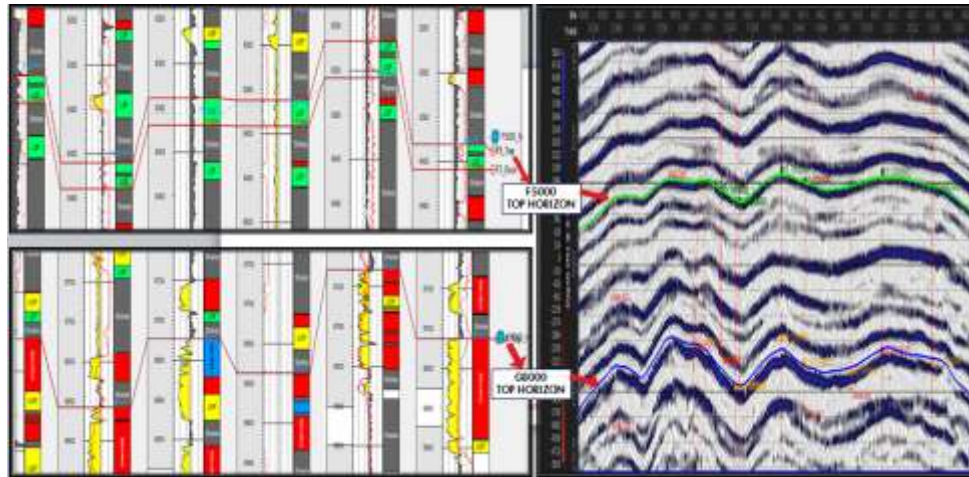


Figure 18: Robustness check of final depth events against well tops (ground truthing reference data).

random noise (incoherent noise) in the seismic volume (Figure 3b).

Prior to well-to-seismic tie stage, this work analysed and quality checked available well data in view of its use to constrain structural interpretation. Fourteen (14) wells penetrated Obom field structure; most wells had incomplete logs including OBOM-001 & OBOM-006 known to have existing Checkshot and sonic logs only but no density information still. This necessitated modelling density after spliced SP and GR logs in order to mitigate the absence of density and radioactive interval existence in F5000 reservoir sand.

OBOM FIELD WELL-TO-SEISMIC TIE

Accurate well-to-seismic tie exercises were performed using reprocessed 3D seismic reflectivity data, Checkshot velocity data, sonic logs, and modelled density logs from Obom-001 and Obom-006 wells which have been quality checked. Synthetic seismogram was computed by convolving dominant frequency of 27hertz wavelet extracted from seismic at well location with the reflectivity coefficients generated from series of acoustic

impedance contrasts built from multiplying Checkshot-calibrated sonic and density. A good tie was achieved after iterative testing of parameters and then applying the best case time bulk shift of 12.4ms and 1.4ms for Obom-001 and Obom-006 wells from shallow to deep section of well-to-seismic tie panel. To further improve the correlation coefficient and match, between the reservoirs top (horizon) identified on wells synthetic and event or loop on seismic, a slight stretch and squeeze was carefully applied within the F5000 and G8000 reservoir time window. This achieve better tie and balanced lobe symmetry of wavelets between synthetic and seismic seismograms. As well, the synthetic seismogram has been flipped by 180 degrees to honour seismic in zero phase.

TIME STRUCTURE MAPS GENERATION/AMPLITUDE EXTRACTION

The grids and surfaces were generated interpreted from horizons which further were used as inputs for amplitude extraction; while logged fluid contacts information were used for quality checking the conformity of amplitude expression with structure including other geological reasoning. The RMS amplitude extraction method was



Figure 19: Logs used to QC the layering of reservoir model for (A) G8000 and (B) F5000.

deployed for the generation of F5000 and G8000 time amplitude structure maps. F5000 amplitude map showed better amplitude expression that was conformable with structure. In the case of G8000 amplitude map, it showed patchy amplitude expression that was seen scattered and not conformable with structure. G8000 reservoir has logged fluid contacts at 9858ft (OWC) and 9797ft (GOC) being a brown reservoir and these were used to constrain the amplitude and depth maps.

TIME-TO-DEPTH CONVERSION

Sequence stratigraphy approach was done to further understand the reservoir properties distribution and depositional environment. It commenced with the identification of key stratigraphic surfaces such as sequence boundary and flooding surfaces. Two sequences were identified between the G8000 and F5000 reservoir in the OBOM field.

FACIES IDENTIFICATION

Due to absence of core data, facies identification was based strictly on log Motifs and side wall sample

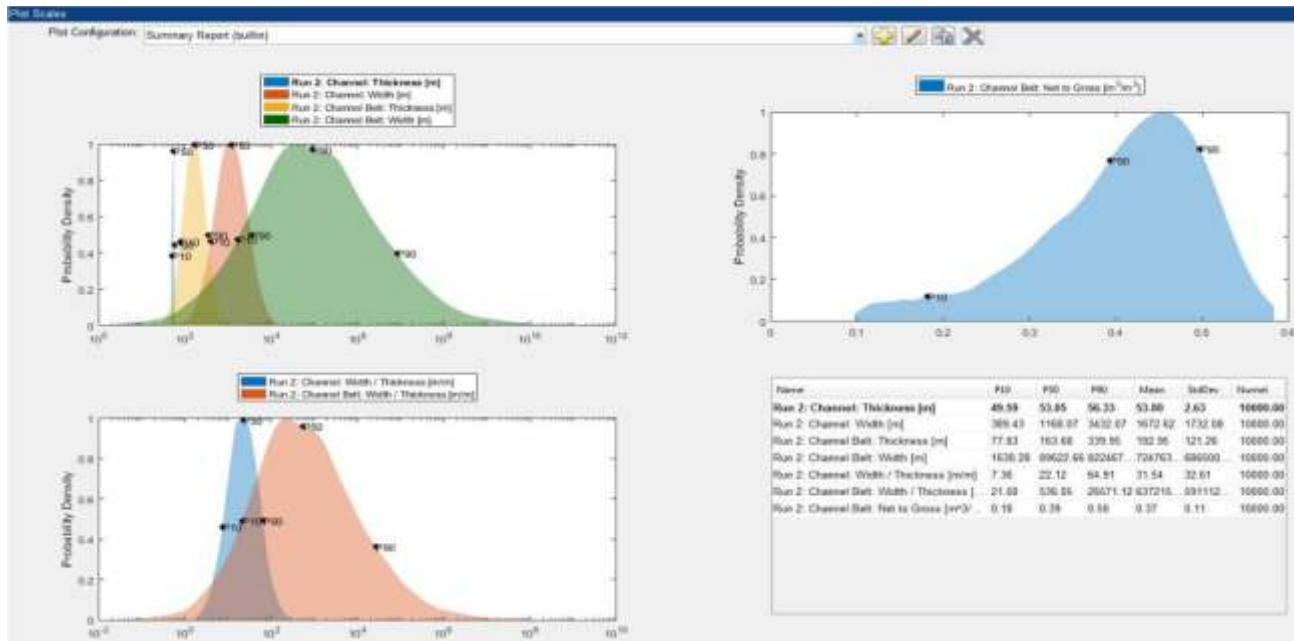


Figure 20: Channel width QA/QC using the STAT tool.

Multi-Velocity modelling was performed for conversion of Time interpreted seed grids to depth domain where it is useful for further subsurface evaluations. Three (3) Velocity models were built using seismic & well velocities (calibrated sonic using Checkshot in OBOM - 001 & -006 respectively); these included 3D seismic velocity model, V0K and Polynomial (2nd order function) model. Harmonized Well tops (Markers) at well penetrations were used to constrain the models after depth conversion.

STRATIGRAPHIC CORRELATION/SEQUENCE STRATIGRAPHY

The stratigraphic correlation for the G8000 reservoir was done by using gamma ray logs, density logs and resistivity logs trending in west – east direction(W-E) along strike showing the lateral continuity of reservoir and north-south in the dip direction. While for the F5000 reservoir was done using a combination of SP log, resistivity logs, and density logs as this was radioactive sand and could not be delineated with the gamma ray log.

description where Fining upward sequences were taken to be channel systems, Blocky signature were taking also as channel and coarsening upward sequences (funnel shape) were taken to be shoreface systems (Cant, 1992). Further subdivision into channel and channel heterolith and lower and upper shoreface was based on the how clean the sand packages.

STATIC MODELLING

A detailed workflow was employed into building the Static model.

RESULTS AND DISCUSSION

FACIES IDENTIFICATION/ STRATIGRAPHIC CORRELATION

Five facies type were identified in the G8000 which includes channel sands, Upper shoreface and shales and in the F5000 reservoir facies includes Lower shoreface, and shales.

A field wide correlation, correlation along strike using wells OBOM-006, OBOM-012, OBOM- 001 and

OBOM-002 and in the dip direction using Wells OBOM-012, OBOM-003 and OBOM-008 respectively was carried out, by integrating gamma ray, spontaneous potential (SP), resistivity logs and density; tops and bases of the two reservoirs of interests were mapped. The occurrence and distribution of the lithostratigraphic units appear to reflect influence of basin morphology and sea level rise. The reservoirs appeared to be continuous across the wells and sand thickness reducing in the West to East direction while the shale increase in the dip direction (distal) as characteristics of the Niger Delta.

SEQUENCE STRATIGRAPHY

Two 3rd Order depositional cycles were identified (SQE1 and SQE2) and the associated system tracts in the OBOM field based from the G8000 sand to the F5000 sand. It is

noticed that reservoir thickness reduces from the bottom ups and the proximal channel sands gradually overlain by upper shoreface sands and lower shoreface sands at the F5000. This is typical of a transgressive marine setting.

CONCEPTUAL MODEL

The integration of well logs correlation, sequence stratigraphy, biostratigraphic data, Side Wall Sample description and desktop studies indicates that the G8000 reservoir was deposited in a channelized shoreface setting in a coastal/ marginal marine setting (Middle to outer Neritic marine) (Figure a). The sedimentary setting is predominantly deltaic and comprises of tidal channels and shoreface. The F5000 reservoir at a shallower section was deposited in a lower shoreface environment (Figure b).

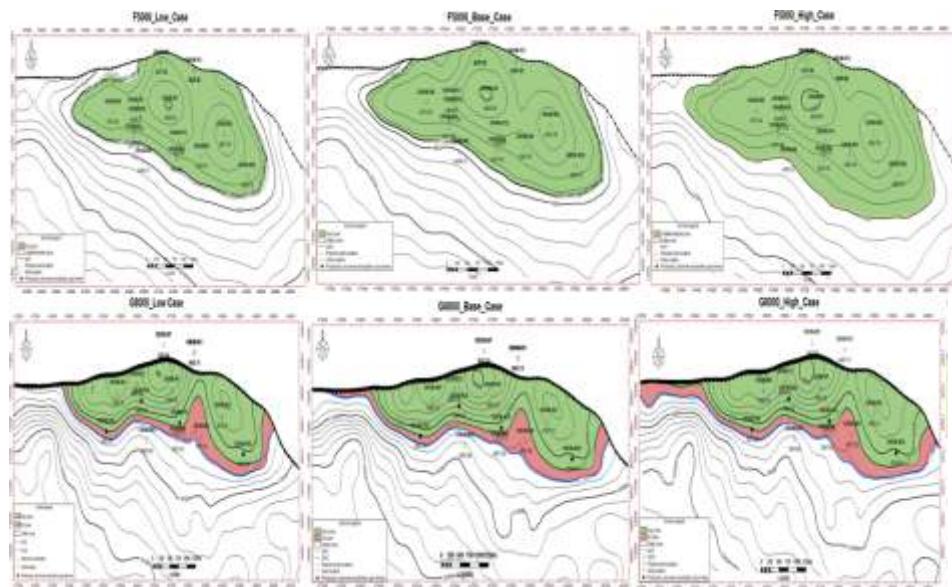


Figure 21: Realizations of top structure maps showing the low, base and high cases.

Table 4: showing the estimated Volumetrics for both reservoir.

Reservoir	Fluid Type	Contacts [ft.]			Net to Gross			POR (%)	SAT (%)	Volumes		
		LC	BC	HC	LC	BC	HC			LC	BC	HC
G8000	Oil (MMstb)	OWC -9858	OWC -9858	OWC = -9858	0.92	0.97	0.99	23	4.7	40	47	52.8
G8000	Gas (Bscf)	GOC -9797	GOC -9797	GOC -9797	0.92	0.97	0.99	23	87	232	261	309
ARPR 2017 for oil										31.2	44	60.70
ARPR 2017 for gas										172	240	320
F5000	Gas (Bscf)	GDT = -8441	Midway = -8469.5	WUT = -8498	0.69	0.77	0.99	11	12.9	29.3	37.4	51.74
ARPR 2017											19	

WELL-TO-SEISMIC TIE

Well-tie matrix scoring guide catalogue was used to judge the seismic-well tie quality. From which satisfied result was justified and accepted and then updated TZ function was saved and outputted for velocity modelling. Table 1 shows the scoring template.

REFLECTION PATTERN ANALYSIS (GEOLOGICAL CONFIRMATION)

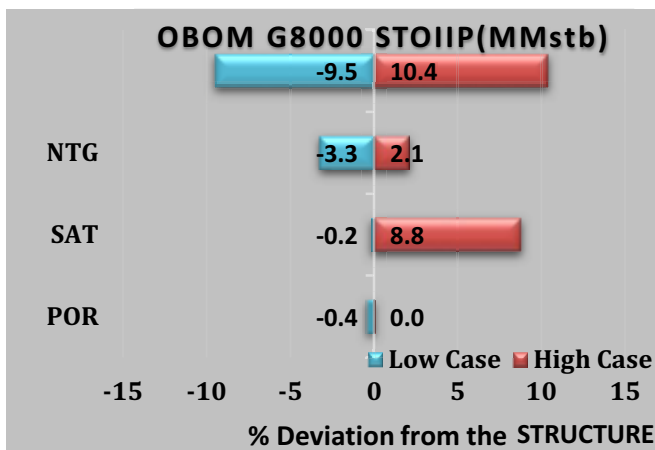


Figure 22: Tornado plot for G8000 reservoir.

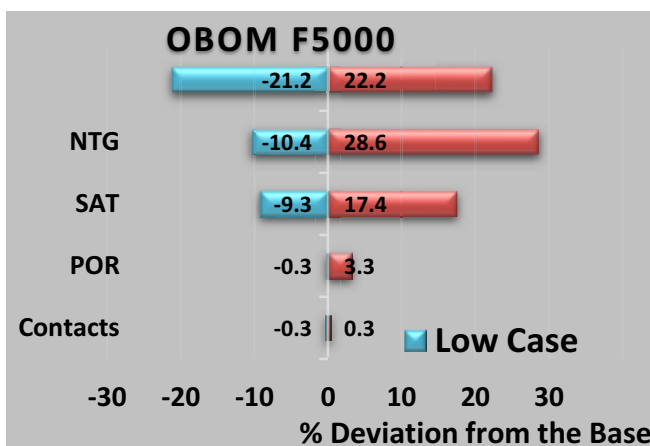


Figure 23: Tornado plot for F5000 reservoir.

The concept of Reflectivity Pattern Analysis (RPA) applied in the Obom field was a forward modeling operation to predict seismic response from formation tops. As mentioned earlier, a synthetic seismogram was matched to a real seismic trace and from which the horizons of interest were interpreted. Input for this included sonic, modelled density and gamma ray logs. RPA analysis showed F5000 Formation Top of reservoir sand on well corresponded (match alignment) to

acoustically soft kick on the Reflection Coefficient (RC) series and peak amplitude on synthetic for both reservoirs.

FAULT INTERPRETATION

The OBOM field faults were interpreted using the van Gogh filtered 2016 reprocessed 3D PSDM seismic volume together with the seismic semblance volume generated. The fault interpretation was carried out in two phases with emphasis on the structural styles and sealing of fault-horizon intersections. Firstly, a total of eight (8) fault segments were interpreted over the OBOM seismic survey area in time domain, with close attention paid to the major north bounding growth fault (Cyan fault). This mapped fault (Cyan) defined the field trapping system morphology and hydrocarbon accumulation as a simple rollover anticlinal structure having majorly a 3-way closure that is fault assisted. No evidence of intra-reservoir compartmentalization from the seismic resolution and semblance volume within the reservoir level of interest. This is supported by the simple nature of the field as a simple rollover structure that is assisted by syn-depositional phase faulting which trended East-West and South-hading direction in the Greater Ughelli depobelt.

HORIZON INTERPRETATION OF F5000 AND G8000 RESERVOIRS

In total two horizons (F5000 and G8000) were interpreted across the 3D PSDM van Gogh filtered seismic cube. Reflectivity Pattern Analysis (RPA) seismic signature overlain on the seismic volume guided in the mapping of the horizons from the well location. To ensure accuracy, the two horizons were picked on a field seed grid defined by 4-lines interval in the crossline and inline directions of the seismic section. The planar display of semblance guided extent of the seed grids. The boundary was limited by the bounding growth fault to the north. The seismic and structural character of the mapped horizons is summarised below:

F5000 (shallower) horizon: F5000 reservoir top showed laterally reflector continuity and exhibits strong amplitude expression within the anticlinal closure (on-structure). F5000 horizon structure has well developed dip closures assisted by fault, with ridges and saddles properly mapped.

G8000 (deeper) horizon: G8000 reservoir top showed fairly laterally reflector continuity and exhibits weak to